International Journal of Pure and Applied Physics. ISSN 0973-1776 Volume 13, Number 1 (2017), pp. 17-20

ON THE RELATIVE ROLE OF TEMPERATURE OF FRAGMENTS WITHIN THE FRAMEWORK OF QUANTUM MOLECULAR DYNAMICS MODEL

Rohit Kumar[1], Arun Sharma[2], Samiksha Sood[3] and Rajeev K. Puri[3]

***Abstract*— We study the role of different temperatures of fragmenting system on the final cluster structures by using quantum molecular dynamics (QMD) model as a tool to generate the phase space of nucleons and minimum spanning tree with binding energy constrain as a cluster recognition algorithm. Different values of temperature are included in the temperature-dependent binding energies to check the sensitivity. We found a significant dependence of fragment structures on the temperature one is using. We also compare our results with experimental data and observe consistent results.**

***Index Terms*—Dynamical models, clusterization algorithm, temperature-dependent binding energies, role of temperature.**

I. INTRODUCTION

Multifragmentation phenomenon [1–6] in heavy-ion collisions is a complex dynamic process that needs in principle, a sophisticated treatment. During last three decades, promising theoretical approaches [7–9] have given us valuable information about the dynamics of the formation of complex clusters. But very few dynamical descriptions exist in the literature that includes the relevant aspects of cluster formation, such as nuclear binding energy, density and excitation of the fragmenting system [7-18]. For example, in some of the studies, stability of the clusters is checked by applying "cold" binding energy criteria [10-14]. At the same time, one is also aware of the fact that these clusters are not cold; instead are excited [19-23]. This fact questions the applicability of these studies involving cold binding energies.

In another study [18], it was considered that the excited clusters will emit secondary particles until they cool down to nearly zero excitation, even though the low energy physics clearly shows that the nucleus can sustain or remain stable up to temperature of few MeVs [24-26]. Keeping this in mind, recently, we used temperature-dependent binding energies to filter out unstable clusters and found several interesting aspects when temperature of fragmenting system was considered to be 4 MeV. This implementation was made in the minimum spanning tree (MST) clusterization algorithm which is based on the spatial correlations among nucleons. We found that this extended algorithm (dubbed as MST-BT) can provide realistic cluster structures quite early in the time. As mentioned above, we take fix temperature of 4 MeV in these studies. At the same time, we also understand that the temperature of the fragmenting system cannot be constant, rather it can vary from cold (T = 0 MeV) to 4-6 MeVs [19-23]. Therefore, here we extend our previous studies by varying the temperature of the fragmenting system between 0 and 4 MeV. Note that, we limit our study upto 4 MeV temperature, as no temperature-dependent formula is available that produces binding energies above this temperature [24-26].

First, in section II, we will present details and approximations of the clusterization algorithm to obtain realistic clusters. Thereafter, the effect of different temperatures on the cluster structures will be presented in section III. We will compare our results with experimental data in section IV. Lastly, we will conclude our study in section V.

II. CLUSTERIZATION ALGORITHM: EXTENDED MINIMUM SPANNING TREE

The initial information about the evolution of the nucleus-nucleus collision is generated using quantum molecular dynamics (QMD) model. The information is in the form of phase space of the nucleons and is stored at number of time steps depending upon the problem in hand. For the details of the QMD model, reader is referred to Ref. [7]. From the phase space of the nucleons, the pre-clusters are obtained by regarding coordinate space correlations among the nucleons using minimum spanning tree (MST) method [7]. This method defines the nucleons to be part of the same cluster if they are closer than 4 fm. Although, this method defines the clusters in the simplest way and is very fast in numerical realization, the clusters can be identified only if they are sufficiently well separated in the coordinate space. Moreover, the obtained clusters may be filamented/excited. To take care of this aspect, each cluster is supplemented to temperature-dependent binding energy criteria. For each pre-cluster, binding energy is calculated as the sum of the potential and kinetic energies of the constituting nucleons with respect to the center-of-mass of the pre-cluster. According to the new definition of a cluster [15], a set of nucleons are part of the same cluster A_f, if binding energy of each cluster (ς) satisfies the following condition:

[1]Department of Physics, Dayanand Anglo-Vedic College, Chandigarh -160 010. (corresponding author e-mail: rohitksharma.pu@gmail.com)
[2]G. D. College, Thanna Mandi, Rajouri, Jammu and Kashmir-185212.
[3]Department of Physics, Panjab University, Chandigarh-160014.

$$\varsigma < E_{Bind}^{Thermal},$$

where

$$\varsigma = \sum_{i=1}^{A_f}\left[\frac{\left(\vec{p}_i - \vec{p}_f^{\,cm}\right)^2}{2m} + \sum_{i<j}^{A_f} V_{ij}\right], \quad (1)$$

where $\vec{P}_f^{cm}$ represents the centre-of-mass momentum of each pre-cluster and V_{ij} is the interaction energy between the constituting nucleons of that cluster. The value of $E_{Bind}^{Thermal}$ is calculated using the formula given by [24]

$$E_{bind}^{Thermal}(T) = \alpha(T)A_f + \beta(T)A_f^{2/3} + \left(\gamma(T) - \frac{\eta(T)}{A_f^{1/3}}\right)\frac{(4t_\varsigma^2 + 4\,|\,t_\varsigma\,|)}{A_f}$$
$$+ 0.8706\frac{Z_f^2 R(0)}{A_f^{1/3}R(T)}\left(1 - \frac{0.7636}{Z_f^{2/3}} - 2.29\frac{R(0)^2}{[R(T)A_f^{1/3}]^2}\right) + \delta(T)\frac{f(A_f, Z_f).}{A_f^{3/4}} \quad (2)$$

Here, Z_f and A_f denote the charge and mass number of each pre-cluster. In the present case, the above formula will be used at different temperatures of 0, 1, 2, 3 and 4 MeVs. The values of the parameters used in the above formula (eq. 2) are temperature-dependent and have been extracted from the graphical representation of Ref. [24]. The implementation of the binding energy criteria at T = 0, 1, 2, 3 and 4 MeVs in MST-BT formalism will be represented as MST-BT (1.0), MST-BT (1.1), MST-BT (1.2), MST-BT (1.3) and MST-BT (1.4), respectively.

III. Results and Discussion

In Fig. 1, we display the time evolution of the mean size of the largest fragment $<A^f_{max}>$ and multiplicity spectrum of free nucleons (FNs), light charged particles (LCPs) [$2 \le A_f \le 4$], and intermediate mass fragments (IMFs) [$5 \le A_f \le 44$] for the central reactions of $^{84}Kr+^{197}Au$ at incident energies of 55 (left panels) and 200 MeV/nucleon (right panels). The results obtained using MST-BT (1.0), MST-BT (1.1), MST-BT (1.2), MST-BT (1.3) and MST-BT (1.4) are denoted by solid, dash-dot, dash-dot-dot, short dash-dot and dashed lines, respectively.

In the initial stage of the reaction, projectile and target collide to form a highly excited compressed composite system. At this stage of the reaction (approximately upto 70 (50) fm/c at an incident energy of 55 (200) MeV/nucleon), the system is highly unstable, therefore, almost all the pre-clusters fail to fulfill binding energy criteria corresponding to any temperature. As a result, no cluster can be seen and hence almost all the nuclear matter appears in the form of free nucleons. After this stage, the compressional energy stored in the system forces the nuclear matter to expand or cool down

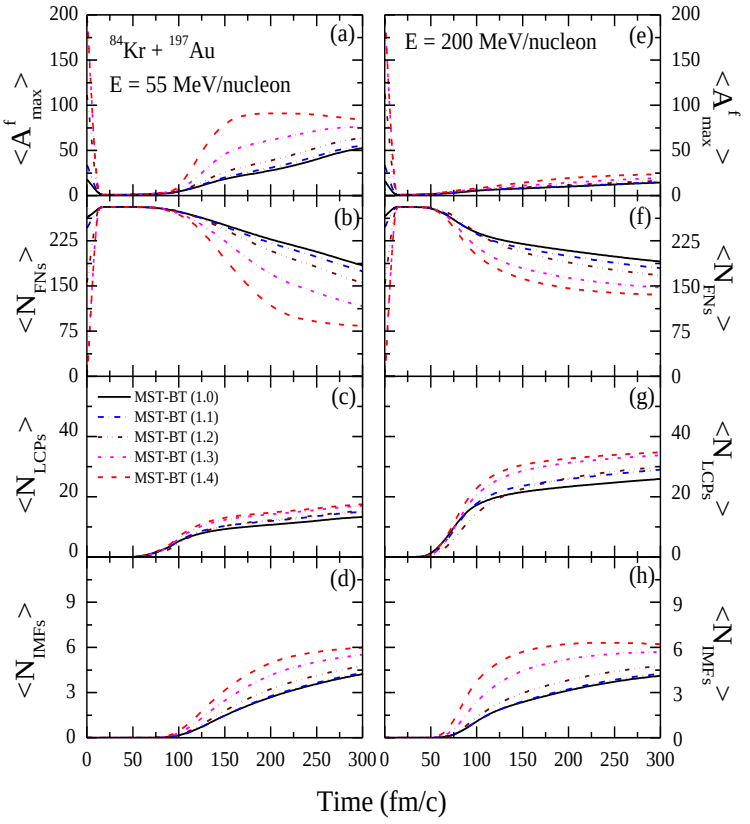

Fig.1. The time evolution of the mean size of the largest fragment $<A^f_{max}>$ and multiplicities of FNs, LCPs and IMFs for the central reactions of $^{84}Kr+^{197}Au$ at incident energies of 55 (left panels) and 200 MeV/nucleon (right panels). The results obtained using MST-BT (1.0), MST-BT (1.1), MST-BT (1.2), MST-BT (1.3) and MST-BT (1.4) are denoted by solid, dash-dot, dash-dot-dot, short dash-dot and dashed lines, respectively.

and clusters are now able to fulfill binding energy constraints. This leads to identification of bound clusters and multiplicities of the clusters starts to increase and free nucleons starts to decrease.

From the figure, we see that lesser (greater) number of clusters is found as bound clusters (free nucleons) with MST-BT (1.0) compared to MST-BT (1.4) or any other version. This happens because with the rise in the temperature, the binding energy of nuclei decreases or clusters need to pass lesser stiff binding energy check to be identified as bound structure. At the same time, we also observe that the use of different temperatures in the MST-BT formalism changes the final fragment structures to great extent. Thus, one should be very careful in using the values of the temperature of the fragmenting system in MST-BT formalism to get realistic clusters.

Next, in Fig. 2, we display the sum of the charges of the bound clusters $<Z_{bound}>$ (defined as the sum of the charges of the clusters with $Z_f \ge 2$) [6] at freeze out time (300 fm/c). We can see that larger number of clusters appear as bound clusters at lower incident energy of 55 MeV/nucleon compared to 200 MeV/nucleon. This happens due to the reason that as the

incident energy is increased, the excitation energy stored in the colliding system increases, causing the increase in the breaking of the system. Therefore, lesser number of clusters is identified as bound at higher energies. We can also observe the same results as in Fig. 1 at final times; maximum number of bound clusters with MST-BT (1.4) method compared to other versions of MST-BT; as clusters have to fulfill lesser binding energy cuts. We also observe a significant difference in the $<Z_{bound}>$ values with different versions of MST-BT. These results point toward the importance of including actual temperature of the fragmenting system, while identifying stable/realistic clusters.

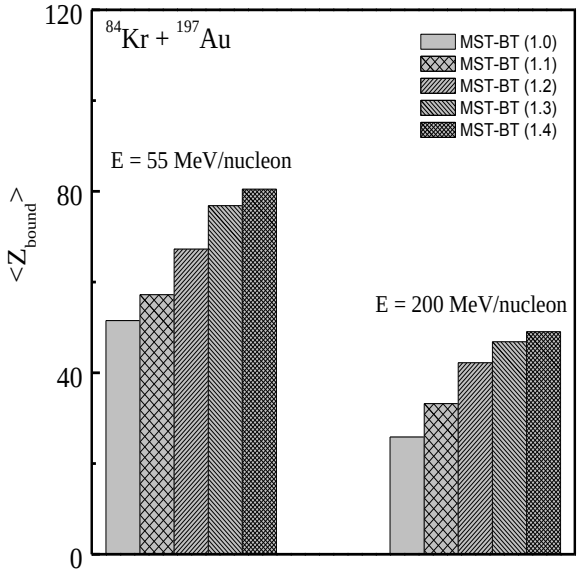

Fig.2. Same as Fig.1, but for the sum of the charges of the clusters identified as bound ($<Z_{bound}>$) at freeze out time.

IV. COMPARISON WITH EXPERIMENTAL DATA

Lastly, in Fig. 3, we compare our results of IMFs and charge particle multiplicity ($<N_C>$) obtained using different versions of MST-BT with experimental data [6] of the central reactions of ^{84}Kr+^{197}Au as a function of projectile incident energy. The experimental data is shown by stars, and the results obtained using MST-BT (1.0), MST-BT (1.1), MST-BT (1.2), MST-BT (1.3) and MST-BT (1.4) are denoted by squares, circles, triangles, inverted triangles and diamonds, respectively. Experimentally, it was observed that the IMF multiplicity increases upto certain energy then it has steady fall out.

In contrast, the values of $<N_C>$ show monotonic increasing trend throughout the energy range. From the figure, we see that our calculated results with all versions of MST-BT are in agreement with experimental results at least qualitatively. Before comparing the quantitative values, we should mention that the role of filters is not included in theoretical calculations [27], therefore, it may give a false expression; that theoretical calculations deviate drastically compared to experimental values. Also as the light charged particles have major

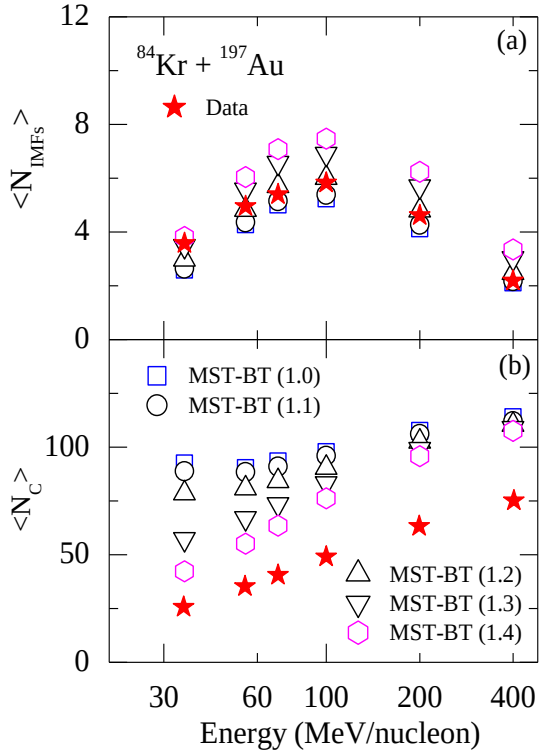

Fig.3. The values of IMFs (Upper panels) and the charge particle multiplicities of bound clusters $<N_C>$ (lower panel) as a function of incident energy of the projectile for the central reactions of ^{84}Kr+^{197}Au . The experimental data is represented as stars [6], whereas other symbols are described in text.

contribution from participant region or equilibrated region, their emission is uniform in all directions; causing the large number of charged particles get lost in the beam direction. Adding to this many particles may not be detected due to multi-hit events. This causes the theoretically observed values of $<N_C>$ to greatly exceed the experimental ones. Thus, we are only able to reproduce the general trend of the $<N_C>$ and not exact values. On the other hand, the effect of filters is lesser on the multiplicities of IMF, therefore, our calculations can be compared to experimental data. We see that experimental values of IMF multiplicities lie in between MST-BT (1.0) and MST-BT (1.4). This reflects the fact that including the temperature of the fragmenting system leads to increase in the compatibility of our calculations with experimental values. Further, it is very important to mention here that these results may get modified if exact temperature of individual cluster will be included in the MST-BT formulation as compared to considering the whole fragmenting system at constant value. The work is in progress in this direction.

V. SUMMARY

In this study, we discuss the effect of the temperature of fragmenting system by incorporating the thermal binding energies at different temperatures. Here thermal binding energies were implemented in minimum spanning tree method. We studied this aspect by including temperature-dependent binding energies at different temperatures in the extended minimum spanning tree method. We observed a significant role of inclusion of different temperatures in the clusterization algorithm on the final cluster structures. We have also shown that the comparison of theoretical data with experimental data will be more appropriate, if temperature of each cluster will be included.

REFERENCES

[1] A. Schuttauf *et al.,* "*Universaility of spectator fragmentation at relativistic bombarding energies*", Nucl. Phys. A **607**, 457 (1996).
[2] M. B. Tsang *et al.,* "*Onset of Nuclear Vaporization in ^{197}Au+ ^{197}Au Collisions*", Phys. Rev. Lett. **71**, 1502 (1993).
[3] W. Bauer, G. F. Bertsch, W. Cassing, and U. Mosel, "*Energetic photons from intermediate energy proton- and heavy-ion-induced reactions",* Phys. Rev. C **34**, 2127 (1986).
[4] R. Ogul *et al.,* "*Isospin-dependent multifragmentation of relativistic projectiles*", Phys. Rev. C **83**, 024608 (2011).
[5] T. Li *et al.,* "*Intermediate Mass Fragment Production in Central Collisions of Intermediate Energy Heavy Ions*", Phys. Rev. Lett. **70**, 1924 (1993).
[6] G. F. Peaslee *et al.,* "*Energy dependence of multifragmentation in ^{84}Kr + ^{197}Au collisions*", Phys. Rev. C **49**, R2271 (1994).
[7] J. Aichelin, "*Quantum molecular dynamics: A dynamical microscopic n-body approach to investigate fragment formation and the nuclear equation of state in heavy-ion collisions",* Phys. Rep. **202**, 233 (1991).
[8] S. R. Souza *et al.,* "*Probing the symmetry energy from the nuclear isoscaling*", Phys. Rev. C **78**, 014605 (2008).
[9] B. Borderie, M. F. Rivet, "*Nuclear multifragmentation and phase transition for hot nuclei*", Prog. Part. and Nucl. Phys. **51**, 551 (2008).
[10] S. Kumar and R. K. Puri, **"***Role of momentum correlations in fragment formation*" Phys. Rev. C **58**, 320 (1998).
[11] C. Dorso and J. Randrup, "*Early recognition of clusters in molecular dynamics model*", Phys. Lett. B **301**, 328 (1993).
[12] J. Singh and R. K. Puri, "*Study of the formation of fragments with different clusterization methods*" J. Phys. G: Nucl. Part. Phys. **27**, 2091 (2001).
[13] S. Kumar and R. K. Puri, "*Stability of fragments formed in the simulations of central heavy ion collisions*" Phys. Rev. C **58**, 2858 (1998).
[14] S. Goyal and R. K. Puri, "*Formation of fragments in heavy-ion collisions using a modified clusterization method*", Phys. Rev. C **83**, 047601 (2011).
[15] R. Kumar, S. Gautam and R. K. Puri, "*Multifragmentation within a clusterization algorithm based on thermal binding energies*", Phys. Rev. C **89**, 064608 (2014).
[16] R. K. Puri and J. Aichelin, *"Simulating annealing clusterization algorithm for studying the multifragmentation",* J. Comput. Phys. **162,** 245 (2000).
[17] A. Le Fevre, Y. Leifels, J. Aichelin, C. Hartnack, V. Kireyev and E. Bratkovskaya, *"FRIGA, a new approach to identify isotopes and hypernuclei in n-body transport models",* J. Phys.: Conf. Ser. **668**, 012021 (2016).
[18] R. J. Charity *et al.,* "*Systematics of complex fragment emission in niobium-induced reactions*", Nucl. Phys. A **483**, 371 (1988).
[19] J. B. Natowitz *et al.,* " *Caloric curves and critical behavior in nuclei*", Phys. Rev. C **65**, 034618 (2002).
[20] J. Wang *et al.,* "*Tracing the evolution of temperature in near Fermi energy heavy ion collisions",* Phys. Rev. C **72**, 024603 (2005).
[21] A. Barranon, C. O. Dorso and J. A. Lopez, *"Time dependence of isotopic temperatures",* Nucl. Phys. A **791**, 222 (2007).
[22] S. Albergo, S. Costa, E. Costanzo, and A. Rubbino, "*Temperature and free-nucleon densities of nuclear matter exploding into light clusters in heavy-ion collisions*", Nuovo Cimento A **89**, 1 (1985).
[23] F. Hoyle, "*The synthesis of elements from hydrogen, Monthly Notices of the Royle Astronom*" Soc. **106**, 343 (1946).
[24] N. J. Davidson *et al., A semi-empirical determination of the properties of nuclear matter*", Phys. Lett. B **315**, 12 (1993).
[25] M. Pi, X. Vinas and M. Barranco, "*Estimation of temperature effects on fission barriers*", Phys. Lett. B **26**, 733 (1982).
[26] G. Sauer, H. Chandra and U. Mosel, "*Thermal properties of nuclei",* Nucl. Phys. A **264**, 221 (1976).
[27] P.-B. Gossiaux and J. Aichelin, *"Importance of initial-final state correlations for the formation of fragments in heavy ion collisions",* Phys. Rev. C **56**, 2109 (1997).